

UNCLASSIFIED

AD 414386

DEFENSE DOCUMENTATION CENTER

FOR

SCIENTIFIC AND TECHNICAL INFORMATION

CAMERON STATION, ALEXANDRIA, VIRGINIA



UNCLASSIFIED

NOTICE: When government or other drawings, specifications or other data are used for any purpose other than in connection with a definitely related government procurement operation, the U. S. Government thereby incurs no responsibility, nor any obligation whatsoever; and the fact that the Government may have formulated, furnished, or in any way supplied the said drawings, specifications, or other data is not to be regarded by implication or otherwise as in any manner licensing the holder or any other person or corporation, or conveying any rights or permission to manufacture, use or sell any patented invention that may in any way be related thereto.

63-4-5

Technical Report 1 | Covering the Period 14 October 1961 to 14 October 1962

VISUAL INFORMATION PROCESSING IN INSECTS

This research was supported by the
Biological Sciences Division, AFOSR,
SRLA
under Contract/Grant

Prepared for:
AIR FORCE OFFICE OF SCIENTIFIC RESEARCH
OFFICE OF AEROSPACE RESEARCH
WASHINGTON 25, D.C.

CONTRACT AF 49(638)-1112

By: James C. Bliss

Scale 4

414386

FILE COPY

414386

STANFORD RESEARCH INSTITUTE





November 1962

(2) ORIGINAL CONTAINS COLOR PLATES: ALL DDC REPRODUCTIONS WILL BE IN BLACK AND WHITE. ORIGINAL MAY BE SEEN IN DDC HEADQUARTERS.

Technical Report 1 | Covering the Period 14 October 1961 to 14 October 1962

① VISUAL INFORMATION PROCESSING IN INSECTS,

7 NA
② NA

Prepared for:
AIR FORCE OFFICE OF SCIENTIFIC RESEARCH
OFFICE OF AEROSPACE RESEARCH
WASHINGTON 25, D.C.

⑬
CONTRACT AF 49(638)-1112

⑩
By: James C. Bliss

SRI Project No. 3853

⑨ Rept for 14 Oct 61-17 Oct 62,

⑪ Nov 62,

⑫ H&P

Approved:

⑬ NA

⑭ To Director/Rept 101

Fred J. Kamphorner
F. J. KAMPHORNER, MANAGER CONTROL SYSTEMS LABORATORY

16-19 NA

J. D. Roe
J. D. ROE, DIRECTOR ENGINEERING SCIENCES DIVISION

⑰ 4

BEEPLES

by R. P. Lister

I lie upon my stomach in the grass,
My curious nose two inches from the blades,
And watch the melancholy beetles pass
In the pursuance of their various trades.

Some of them might be monumental masons,
And others warriors equipped for war;
Some might be barbers searching for their basins,
Or longshorebeetles longing for a shore.

I think this beetle either writes or teaches;
His look is anxious and his brow is lined.
And here, behold! a clergybeetle preaches
Damnation to all sinful beetlekind.

Whether I guess correctly there's no knowing;
The ways of beetles are beyond my ken,
But none of them seems certain where he's going—
In this, at least, they're similar to men.

Atlantic, October 1962

ABSTRACT



This report describes mathematical analysis, behavioral experiments, and neurophysiological experiments aimed at determining the mechanisms of visual perception in insects.

The behavioral experiments with the beetle *Lixus* indicate that spatial processing involving autocorrelation is being performed among the ommatidia of the eye. This processing was studied by means of an optomotor reaction involving a turning tendency with movement in the visual field.

Visual processing in the beetle *Lixus* was also studied by means of microelectrode recording of electrical nervous activity. The electroretinogram (ERG) was measured for various visual stimuli and Bode diagrams were determined for small changes in light intensity. Nonlinear effects were also noted for large changes in light intensity.

Spike potentials were obtained from a single cell which fired with a change in light intensity. Spike potentials were also obtained from the ventral nerve cord, anterior thoracic region, and motor nerve stump of the first joint of the right front leg.

A functional model is proposed to explain the behavioral and neurophysiological results.



CONTENTS

ABSTRACT	ii
LIST OF ILLUSTRATIONS	iv
LIST OF TABLES	v
I INTRODUCTION	1
II ECOLOGY AND ANATOMY	3
III FUNCTIONAL MODELS OF THE VISUAL SYSTEM	7
A. Cross-Sectional Models of the Eye	7
B. Two-Ommatidia Functional Model	11
C. Running Autocorrelation	19
IV BEHAVIORAL EXPERIMENTS	21
A. Techniques and Equipment	21
B. Single-Cylinder Experiment	22
C. Double-Cylinder Experiment	24
D. Discussion	25
V ELECTRICAL RECORDINGS FROM THE BEETLE <u>LIXUS</u>	26
A. Methods	26
B. The Electroretinogram (ERG)	26
C. Spike Potentials	34
VI CONCLUSIONS	37
REFERENCES	40
ACKNOWLEDGMENT	41
PROJECT STAFF ACTIVITIES	42

ILLUSTRATIONS

Fig. 1	The Beetle <i>Lixus Blakeae</i> Chittendan. The Average Beetle Is about 1.3 cm long	3
Fig. 2	Ten-Micron-Thick Sections of the Head of a Beetle <i>Lixus</i> . Mallory's Anilin Blue Stain was Used	5
Fig. 3	Angle Estimates Based on the Head Sections of the Beetle <i>Lixus</i>	6
Fig. 4	Functional Diagram Proposed by Reichardt of a Horizontal Section of the Eye	7
Fig. 5	Functional Diagram of Autocorrelation Computer	9
Fig. 6	Function Diagram of a Spectral-Density Computer	10
Fig. 7	Reichardt's Minimal Mathematical Model for a Two-Ommatidia System	11
Fig. 8	Beetle and Y-maze Globe at the Center of a Striped Cylinder	21
Fig. 9	Reaction Versus Cylinder Speed for Various Black and White Stripe Wavelengths	23
Fig. 10	Experimental Setup for the Double-Cylinder Experiment	24
Fig. 11	Stimulus Light Pulse Produced by Strobotac. Horizontal Scale: 20 msec/cm	27
Fig. 12	ERG Response to Strobotac Light Pulse for Repetition Frequency of 100 Pulses Per Minute. Horizontal Scale: 20 μ sec/cm	28
Fig. 13	ERG Response to Strobotac Light Pulse for Pulse Repetition Frequency of 600 Pulses Per Minute. Horizontal Scale: 20 msec/cm	29
Fig. 14	ERG Response to Step Change in Light Intensity. Horizontal Scale: 25 mm/sec. Glass Micropipette in the Dorsal Margin of the Eye	30
Fig. 15	ERG Response to Step Change in Light Intensity. Horizontal Scale: 25 mm/sec. Tungsten Microelectrode in the Center of the Eye	31
Fig. 16	ERG Response to a Triangular Wave of Light Intensity. Horizontal Scale: 500 msec/cm	31
Fig. 17	ERG Response to a Triangular Wave of Light Intensity. Horizontal Scale: 125 mm/sec	32
Fig. 18	Amplitude of the Triangular Wave ERG Response Versus Frequency for Two Experimental Runs	33
Fig. 19	Phase of the Triangular Wave ERG Response Versus Frequency for Two Experimental Runs	33
Fig. 20	Electrical Network that Approximates the ERG Response	34
Fig. 21	Spike Response to a Triangular Wave of Light Stimulus. Horizontal Scale: 5 mm/sec	34
Fig. 22	Rate of Increase of the Stimulus Light Intensity Versus the Reciprocal of the Time Between Pulses	36
Fig. 23	Model of the Two-Ommatidia System	39

TABLE

Table I Results of the Double Cylinder Experiment 25

I INTRODUCTION

Lister's poem describes similarities between beetles and men. However, as Roeder^{1*} and Vowles² have recently emphasized, the insect nervous system differs from the vertebrate nervous system in several important respects. The major differences are these:

- (1) Insect neurons have a smaller cell body.
- (2) Insect nerve fibers are unmyelinated.
- (3) The insect neuron receives its input entirely over its dendritic surfaces, not over its cell body.
- (4) It is probable that the insect has less nervous integration than the vertebrate.
- (5) The number of insect neurons is strictly limited.
- (6) Nerve systems composed of relatively few large units are common in insects, in contrast to those composed of many small units.
- (7) The central nervous system of insects is arranged so that, the coordinating mechanisms for different types of behavior are distributed in well separated regions.

These differences, together with the fact that insects are numerous, inexpensive, and hardy, make them excellent subjects for study. Their nervous system is readily accessible, their mechanisms are more susceptible to analysis, and their visual system is the basis for rather complex behavior. Studies of visual information processing in insects may lead to the development of a theory for the neural basis for behavior which, in turn, could inspire the development of artificial systems that perform sensory functions.

Hassenstein,³ Reichardt,^{4,5} and Varju⁶ have studied visual motion perception of the beetle *Chlorophanus viridis* by analysis of the optomotor response. In the basic type of experimentation, the experimental animal (e.g., a beetle) is placed at the center of a rotating striped drum. The beetle is rigidly held by his thorax, and a Y-maze globe,

* References are listed at the end of the text.

as shown in Fig. 8, is given him to hold. The strips of the Y-maze globe meet at 120° so that, as the beetle walks (without moving) he repeatedly comes to divisions in his path, which are not in his field of view. The tendency to turn right or left depends upon movement in the visual field. A quantitative measure of the response can be arbitrarily defined as $(W - A)/(W + A)$ where W is the number of choices in the direction of, and A is the number against, the movement in the visual field. This measure can be related to the performance of a postulated mechanism for the perception of movement.

From their behavioral experiments, these investigators have been able to deduce a system model for motion perception. In this model, no physiological interaction exists between ommatidia separated by more than one ommatidium. The stimuli received by the ommatidia are linearly transformed and their interaction in the central nervous system made in accordance with the principle of first-order correlation. This model was able to predict the experimental finding that all visual patterns that differ only by different phase relations of their Fourier components produce the same optomotor response as a function of pattern speed.

The present report describes behavioral and neurophysiological experiments that have been performed to investigate further the mechanisms of visual perception in insects. These experiments, together with the mathematical analysis, represent the first year's research of this continuing program.

II ECOLOGY AND ANATOMY

The experimental animal used in the experiments reported here has been identified by the University of California Entomology Department as the beetle *Lixus blakeae* Chittendan. Figure 1 is a photograph of one of these animals. The beetles were collected in Lake Lagunita and Searsville Lake, Palo Alto, California, between May and October 1961 and 1962. They were found on *Polygonum mhlenbergii*, which grows in and around the water. The leaves and stems of this plant are the only acceptable food for these beetles that we have found.



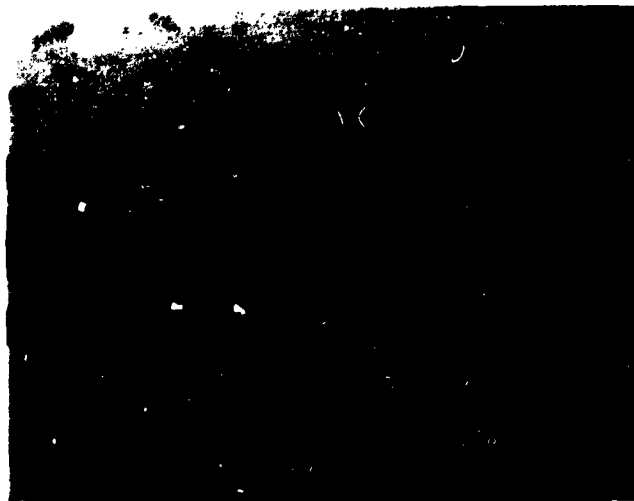
CP-5063-19

FIG. 1 THE BEETLE *LIXUS BLAKEAE* CHITTENDAN
(The average beetle is about 1.3 cm long)

The beetles probably overwinter as pupae in the stems or roots of *Polygonum*. There are probably two generations per year, a short one lasting during the summer with larval stage about two months, and a winter generation in which the larvae may last over six months.

We have been able to keep specimens alive over the winter months by either feeding them leaves of *Polygonum* (some of which had been frozen) or by putting the animals in an air-tight box and keeping it at about 40°F.

Several beetles were sectioned and stained to obtain anatomical information, such as the ommatidial angle, the direction of view of the eye, and the location of the optic lobes. Figure 2 shows several photographs of these sections. Figure 3 shows estimates of pertinent angles based on the sections. The ommatidial angle, or angle between the center lines of adjacent ommatidia, is about 4° and the angle between the center lines of the outermost ommatidia in this plane is about 110°.



250 μ



100 μ

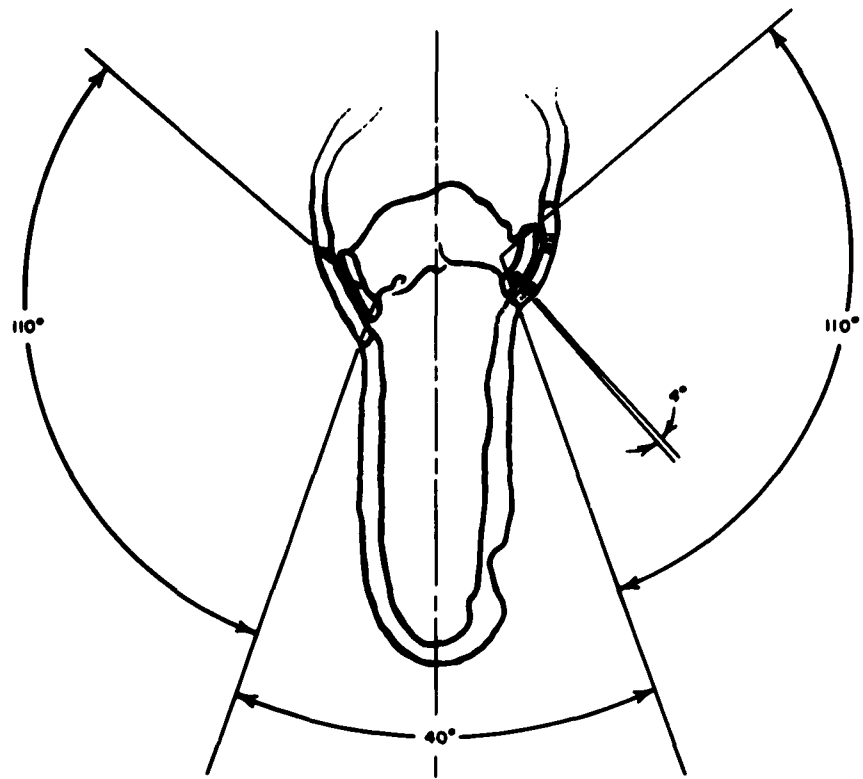


25 μ



25 μ

FIG. 2 TEN-MICRON-THICK SECTIONS OF THE HEAD OF A BEETLE *LIXUS*
(Mallory's anilin blue stain was used)



DA-2000-10

FIG. 3 ANGLE ESTIMATES BASED ON THE HEAD SECTIONS OF THE BEETLE *LIXUS*

III FUNCTIONAL MODELS OF THE VISUAL SYSTEM

A. CROSS-SECTIONAL MODELS OF THE EYE

In order to explain the mechanism of movement perception in terms of their experimental results, Reichardt⁴ proposed the functional diagram of a horizontal section of the eye of the beetle *Chlorophanus* shown in Fig. 4. The letters *A*, *B*, *C*, ... symbolize a row of ommatidia,

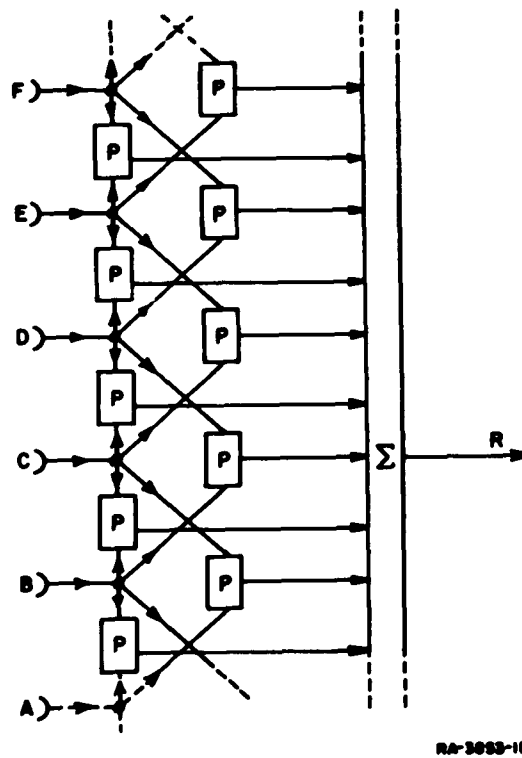


FIG. 4 FUNCTIONAL DIAGRAM PROPOSED BY REICHARDT OF A HORIZONTAL SECTION OF THE EYE

and the connections between ommatidia represent information channels and not actual nerve fibers. The *P* systems perform processing operations upon signals received from pairs of adjacent ommatidia and pairs of adjacent ommatidia once removed. The results of these operations are summed, thus forming the total reaction strength *R*.

If we assume that the P systems perform multiplication, then the functional diagram has a remarkable similarity to a spatial auto-correlation computer. Thus, if we describe the visual field by $f(y, t)$, then an approximation to the spatial autocorrelation function, $\psi(\beta_j, t)$, is

$$\psi(\beta_j, t) = \sum_{i=0}^N f(y_i, t) f(y_i - \beta_j, t) \quad (1)$$

$$\beta_j = 0, c, 2c, \dots$$

where

y_i = the position of the i th ommatidium

t = time

β_j = the shift parameter

c = the center-to-center spacing of the ommatidia

N = the number of ommatidia.

Figure 5 shows a functional diagram representing Eq. (1). Note that, under the assumption that the P systems are multipliers, the functional diagrams of Figs. 4 and 5 are related by

$$R = \psi(c, t) + \psi(2c, t) \quad .$$

Thinking of the eye as an autocorrelation computer suggests an equivalent system to the functional diagram shown in Fig. 5. This equivalent system is based on the spatial spectral density function which is the Fourier transform of the autocorrelation function. Thus, a sampled approximation to the spatial spectral density function $\phi(\omega_k, t)$ is

$$\phi(\omega_k, t) = \frac{1}{4} [a^2(\omega_k, t) + b^2(\omega_k, t)] \quad (2)$$

where ω_k = the k th harmonic of the fundamental spatial frequency,

$$a(\omega_k, t) = \frac{1}{Nc} \sum_{i=0}^N f(y_i, t) \cos \frac{\pi k}{Nc} y_i,$$

and

$$b(\omega_k, t) = \frac{1}{Nc} \sum_{i=0}^N f(y_i, t) \sin \frac{\pi k}{Nc} y_i.$$

Figure 6 shows a functional system that computes $\hat{p}(\omega_k, t)$. The output of this system contains the same information as the autocorrelation system shown in Fig. 5. However, no multipliers are needed (only squarers) in the spatial spectral density system shown in Fig. 6.

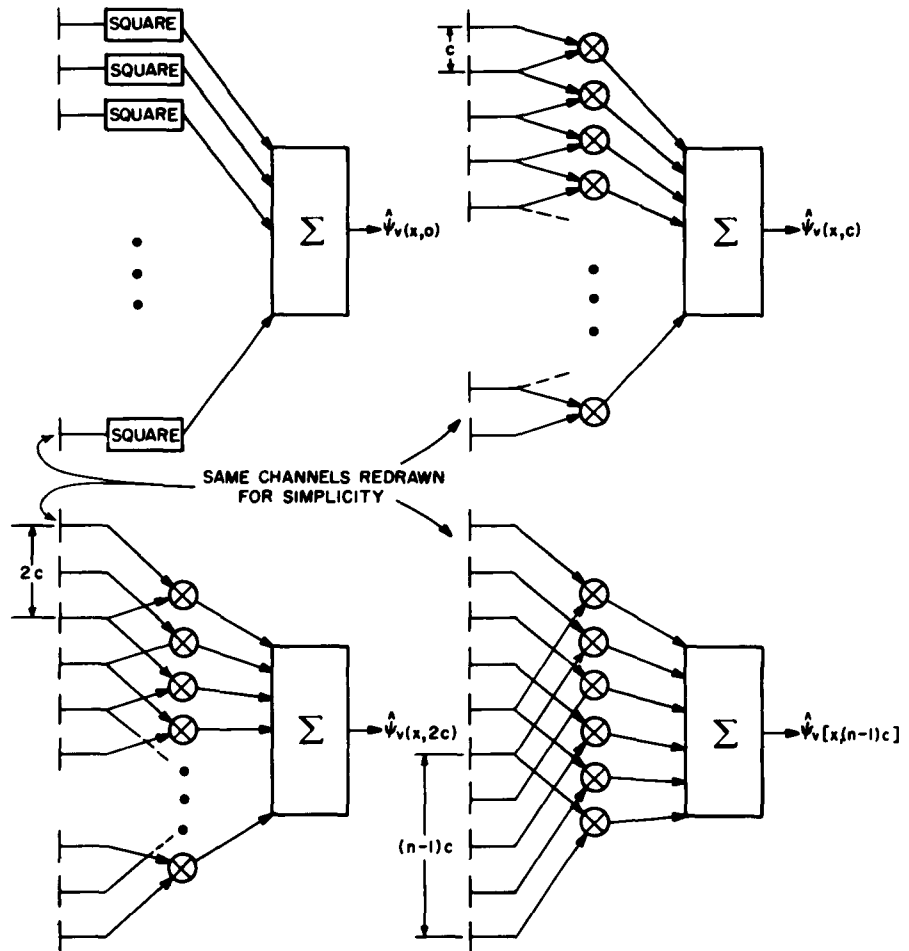


FIG. 5 FUNCTIONAL DIAGRAM OF AN AUTOCORRELATION COMPUTER

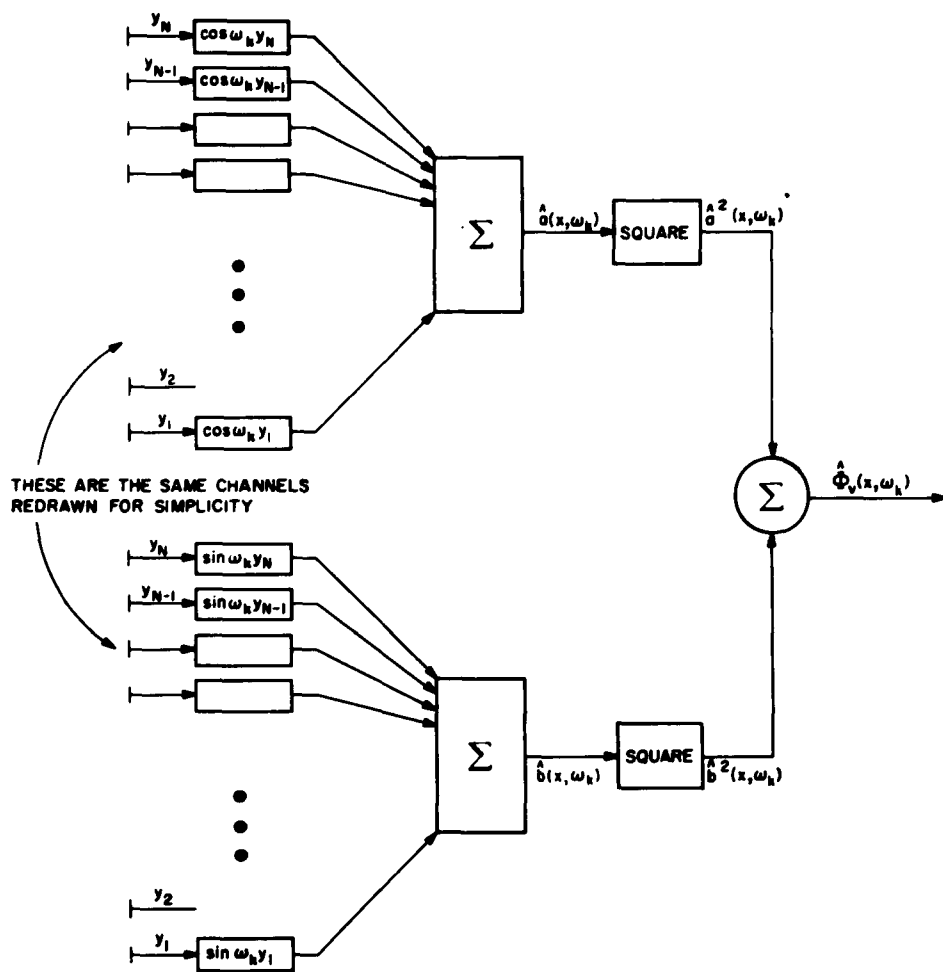


FIG. 6 FUNCTION DIAGRAM OF A SPECTRAL-DENSITY COMPUTER

The relation between the spatial spectral density system and Reichardt's system (shown in Fig. 4 assuming the P systems are multipliers) is

$$\psi(\beta, t) = F^{-1}[\phi(\omega_k, t)]$$

$$R = \psi(c, t) + \psi(2c, t)$$

where F^{-1} signifies the inverse Fourier transform.

B. TWO-OMMATIDIA FUNCTIONAL MODEL

Reichardt⁴⁵ develops the functional structure of the P systems by considering a double system consisting only of ommatidia A and B . Figure 7 shows Reichardt's minimal mathematical model for a two-ommatidia system. Since the development of this model is discussed by Reichardt, only an analysis of the model will be given below.

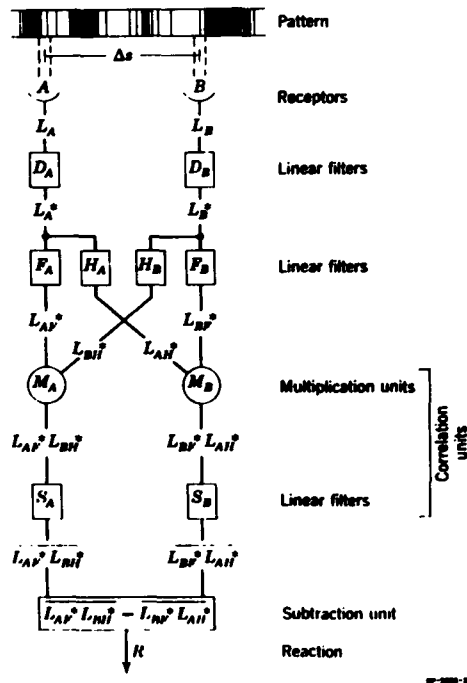


FIG. 7 REICHARDT'S MINIMAL MATHEMATICAL MODEL FOR A TWO-OMMATIDIA SYSTEM

Let L_A be the light intensity received by the A ommatidium and L_B be the light intensity received by the B ommatidium as a function of time. For a pattern moving from left to right

$$L_A = L(t)$$

and

$$L_B = L(t - \Delta t)$$

where Δt is the time it takes a point on the pattern to move from A to B , the ommatidia spacing Δs .

Then, in the time domain, the output of the A multiplier M_A can be expressed as

$$M_A(t) = \left[\int_0^{\infty} W_{DF}(\eta) L(t - \eta) d\eta \right] \left[\int_0^{\infty} W_{DH}(\zeta) L(t - \Delta t - \zeta) d\zeta \right]$$

where

$W_{DF}(t)$ = the weighting function of the D and F filters

$W_{DH}(t)$ = the weighting function of the D and H filters.

If the S filter is a perfect averager (see Sec. III-C), then the output of the S filter is

$$\begin{aligned} \overline{M_A(t)} &= \lim_{T \rightarrow \infty} \frac{1}{2T} \int_{-T}^T M_A(t) dt \\ &= \int_0^{\infty} W_{DF}(\eta) \int_0^{\infty} W_{DH}(\zeta) \psi_{LL}(\zeta + \Delta t - \eta) d\zeta d\eta \end{aligned}$$

where

$$\begin{aligned} \psi_{LL}(\zeta) &= \lim_{T \rightarrow \infty} \frac{1}{2T} \int_{-T}^T L(t)L(t - \zeta) dt \\ &= \text{the autocorrelation function of} \\ &\quad \text{the input pattern.} \end{aligned}$$

Therefore, the output of the model, $R(\Delta t)$, is given by

$$\begin{aligned} \overline{R(\Delta t)} &= \overline{M_A(t)} - \overline{M_B(t)} = \int_0^{\infty} W_{DF}(\eta) \int_0^{\infty} W_{DH}(\zeta) \psi_{LL}(\zeta + \Delta t - \eta) d\zeta d\eta \\ &\quad - \int_0^{\infty} W_{DH}(\eta) \int_0^{\infty} W_{DF}(\zeta) \psi_{LL}(\zeta + \Delta t - \eta) d\zeta d\eta \end{aligned} \quad (3)$$

Equation (3) is a general expression for the output of the two-ommatidia model of Fig. 7 in terms of any input pattern. The corresponding analysis in the frequency domain proceeds as follows:

$$M_A(\omega) = \int_{-\infty}^{\infty} L(\theta) W_{DF}(\theta) L(\omega - \theta) e^{-j(\omega - \theta)\Delta t} W_{DH}(\omega - \theta) d\theta$$

where

$$M_A(\omega) = \text{the Fourier transform of } M_A(t)$$

$$L(\theta) = \text{the Fourier transform of } L(t)$$

$$W_{DF}(\theta) = \text{the Fourier transform of } W_{DF}(t)$$

$$W_{DH}(\theta) = \text{the Fourier transform of } W_{DH}(t)$$

since

$$M_A(t) = M_A(\omega) \Big|_{\omega=0}$$

$$\begin{aligned} \overline{M_A(t)} &= \int_{-\infty}^{\infty} L(\theta) L(-\theta) W_{DF}(\theta) W_{DH}(-\theta) e^{j\theta\Delta t} d\theta \\ &= \int_{-\infty}^{\infty} W_{DF}(\theta) W_{DH}(-\theta) \hat{r}_{LL}(\theta) e^{j\theta\Delta t} d\theta \end{aligned}$$

where

$$\begin{aligned} \hat{r}_{LL}(\theta) &= L(\theta)L(-\theta) \\ &= \text{the power spectral density of} \\ &\quad \text{the input pattern.} \end{aligned}$$

Therefore,

$$R(\Delta t) = \int_{-\infty}^{\infty} [W_{DF}(\theta) W_{DH}(-\theta) - W_{DH}(\theta) W_{DF}(-\theta)] \hat{r}_{LL}(\theta) e^{j\theta\Delta t} d\theta \quad (4)$$

or

$$R(\Delta t) = \int_{-\infty}^{\infty} 2\text{Im}[W_{DF}(\theta) W_{DH}(-\theta)] \hat{r}_{LL}(\theta) e^{j\theta\Delta t} d\theta$$

where $\text{Im} [W_{DF}(\nu)W_{DH}(-\nu)]$ means the imaginary part of $W_{DF}(\nu)W_{DH}(-\nu)$. An alternative expression for $R(\Delta t)$ is

$$R(\Delta t) = 4\pi t^{-1} \{ \text{Im} [W_{DF}(\nu)W_{DH}(-\nu)] \psi_{LL}(\nu) \} .$$

Equation (4) is equivalent to Eq. (3) and gives the output of Reichardt's two-ommatidia model in terms of any input.

In order to understand the general expressions for the output of the two-ommatidia system [Eqs. (3) and (4)], let us consider some special cases:

- (1) Let $\text{Im} [W_{DF}(\omega)W_{DH}(-\omega)] = jK$, where K is a real constant. Then

$$R(\Delta t) = 4\pi K \psi_{LL}(\Delta t)$$

or the output is proportional to the point on the autocorrelation function of the pattern determined by Δt . Since, for a large class of patterns, the autocorrelation function decreases as the shift parameter increases, $R(\Delta t)$ decreases as the velocity of the pattern increases. This principle has been applied in a groundspeed indicator for airplanes.⁷

- (2) Let

$$W_{DF}(\omega) = \frac{1}{\sqrt{4\pi(h-f)}} e^{-j\omega f}$$

and

$$W_{DH}(\omega) = \frac{1}{\sqrt{4\pi(h-f)}} e^{-j\omega h}$$

Then

$$\begin{aligned} R(\Delta t) &= \int_{-\infty}^{\infty} \frac{2j \sin \omega(h-f)}{4\pi(h-f)} e^{j\omega\Delta t} \psi_{LL}(\omega) d\omega \\ &= \frac{1}{2(h-f)} \int_{-\infty}^{\infty} [\mu_0(\tau-h+f) - \mu_0(\tau+h-f)] \psi_{LL}(\Delta t - \tau) d\tau \end{aligned}$$

where $\mu_0(t)$ is the unit impulse function.

$$R(\Delta t) = \frac{\psi_{LL}(\Delta t - h + f) - \psi_{LL}(\Delta t + h - f)}{2(h - f)}$$

or $R(\Delta t)$ is equal to the first difference of the autocorrelation function.

(3) Let

$$W_{DF} = \frac{1}{j\omega} \quad \text{and} \quad W_{DH} = 1$$

Then

$$R(\Delta t) = \int_{-\infty}^{\infty} \frac{2}{j\omega} \phi_{LL}(\omega) e^{j\omega\Delta t} d\omega$$

or

$$R(\Delta t) = 4\pi \int_{-\infty}^{\infty} \psi_{LL}(\Delta t) d\Delta t$$

or $R(\Delta t)$ is equal to the integral of the autocorrelation function.

(4) Let

$$W_{DF} = j\omega \quad \text{and} \quad W_{DH} = 1$$

Then

$$R(\Delta t) = \int_{-\infty}^{\infty} 2j\omega \phi_{LL}(\omega) e^{j\omega\Delta t} d\omega = 4\pi \frac{d\psi_{LL}(\Delta t)}{d\Delta t}$$

or $R(\Delta t)$ is equal to the derivative of the autocorrelation function.

(5) Let

$$W_{DF}(\omega) = \frac{b_{DF} \sqrt{j\omega} e^{-\sqrt{j^a b} \omega}}{a_F + j\omega}$$

and

$$W_{DH}(\omega) = \frac{b_{DH} \sqrt{j\omega} e^{-\sqrt{j^a b} \omega}}{a_H + j\omega}$$

These are the transfer functions proposed by Reichardt.⁴
Thus

$$\begin{aligned} W_{DF}(\omega)W_{DH}(-\omega) &= \frac{-b_{DF}b_{DH}e^{-(1+j)\sqrt{a_D}\omega}}{(a_F + j\omega)(a_H - j\omega)} \\ &= \frac{-b_{DF}b_{DH}j\omega[a_F a_H + \omega^2 - (a_H - a_F)j\omega]e^{-j\sqrt{2a_D}\omega}}{(\omega^2 + a_H^2)(\omega^2 + a_F^2)} \\ \text{Im}[W_{DF}(\omega)W_{DH}(-\omega)] &= \frac{j b_{DF} b_{DH} \omega [(a_F a_H + \omega^2) \sin \sqrt{2a_D}\omega + \omega(a_H - a_F) \cos \sqrt{2a_D}\omega]}{(\omega^2 + a_H^2)(\omega^2 + a_F^2)} \end{aligned}$$

Reichardt⁴ states that $a_D \leq 10^{-4}$ sec. However, note that a_D must equal zero in order for $\text{Im}[W_{DF}(\omega)W_{DH}(-\omega)]$ to approach zero as ω approaches infinity.

$$\text{Im}[W_{DF}(\omega)W_{DH}(-\omega)] = \frac{j b_{DF} b_{DH} \omega^2 (a_H - a_F)}{(\omega^2 + a_H^2)(\omega^2 + a_F^2)} \quad (5)$$

So that

$$R(\Delta t) = \int_{-\infty}^{\infty} \frac{2j b_{DF} b_{DH} \omega^2 (a_H - a_F)}{(\omega^2 + a_H^2)(\omega^2 + a_F^2)} \phi_{LL}(\omega) e^{j\omega\Delta t} d\omega$$

These special cases serve to illustrate that Reichardt's two-ommatidia system computes a function of the autocorrelation function of the input pattern. The actual function of the autocorrelation function computed depends on the transfer functions of the D , H , and F filters. This consideration suggests the possibility of synthesizing W_{DF} and W_{DH} in order to obtain a desired relation between $R(\Delta t)$ and $\psi_{LL}(\Delta t)$. For example, since $\psi_{LL}(\Delta t)$ is closely related to the velocity of the input pattern, one may wish to obtain a linear relation between $R(\Delta t)$ and velocity for a given pattern or given pattern statistics. Such a system could be used as a velocity measuring device. Applications are in noncontact velocity measurement of slurry fluids or ground speed of aircraft.

The synthesis method to obtain W_{DF} and W_{DH} proceeds as follows:

$$R(\Delta t) = 4\pi F^{-1} \{ \text{Im} [W_{DF}(\omega)W_{DH}(-\omega)] \phi_{LL}(\omega) \}$$

$$F[R(\Delta t)] = 4\pi \text{Im} [W_{DF}(\omega)W_{DH}(-\omega)] \phi_{LL}(\omega)$$

$$\text{or } \boxed{\text{Im} [W_{DF}(\omega)W_{DH}(-\omega)] = \frac{F[R(\Delta t)]}{4\pi\phi_{LL}(\omega)}}$$

{Note that $F[R(\Delta t)]$ must be real or $R(\Delta t)$ must be even.} Using the Hilbert transform⁸

$$\boxed{\text{Re} [W_{DF}(\omega)W_{DH}(-\omega)] = -\frac{1}{\pi} \int_{-\infty}^{\infty} \frac{\text{Im} [W_{DF}(\omega_1)W_{DH}(-\omega_1)]}{\omega_1 - \omega} d\omega_1} \quad (7)$$

where Re signifies real part so that

$$W_{DF}(\omega)W_{DH}(-\omega) = \text{Re} [W_{DF}(\omega)W_{DH}(-\omega)] + j \text{Im} [W_{DF}(\omega)W_{DH}(-\omega)]$$

Equations (6) and (7) determine $W_{DF}(\omega)W_{DH}(-\omega)$ in terms of the desired output $R(\Delta t)$ and the input power spectral density $\phi_{LL}(\omega)$.

So far we have considered the relation between the output of the two-ommatidia system and the transfer functions of the D , F , and H filters. Next, some special cases of input patterns will be considered.

(1) If the input pattern can be described by $P(x)$, where

$$P(x) = a \cos \frac{2\pi}{\lambda} x$$

then

$$L(t) = b \cos \omega_0 t$$

where the velocity v of the pattern is

$$v = \frac{\Delta s}{\Delta t} = \frac{\lambda \omega_0}{2\pi}$$

Thus

$$L(\omega) = \frac{b}{2} \left[\mu_0 \left(\omega - \frac{2\pi v}{\lambda} \right) + \mu_0 \left(\omega + \frac{2\pi v}{\lambda} \right) \right]$$

so that

$$\phi_{LL}(\omega) = \frac{b^2}{4} \left[\mu_0 \left(\omega - \frac{2\pi v}{\lambda} \right) + \mu_0 \left(\omega + \frac{2\pi v}{\lambda} \right) \right]^2$$

Substituting into Eq. (4) gives

$$R(\Delta t) = \frac{b^2}{2} \text{Im} \left[\mathbb{H}_{DF} \left(\frac{2\pi v}{\lambda} \right) \mathbb{H}_{DH} \left(-\frac{2\pi v}{\lambda} \right) \right] \left[e^{j2\pi\Delta s/\lambda} - e^{-j2\pi\Delta s/\lambda} \right] \quad (8)$$

$$R(\Delta t) = -jb^2 \text{Im} \left[\mathbb{H}_{DF} \left(\frac{2\pi v}{\lambda} \right) \mathbb{H}_{DH} \left(-\frac{2\pi v}{\lambda} \right) \right] \sin \frac{2\pi\Delta s}{\lambda}$$

Thus for a cosinusoidal input pattern, the output is proportional to $\text{Im} \{ \mathbb{H}_{DF}(2\pi v/\lambda) \mathbb{H}_{DH}(-2\pi v/\lambda) \}$ multiplied by a constant independent of velocity. This constant may be positive or negative and is determined by the contrast of the pattern b , the omnidirectional distance Δs , and the wavelength of the pattern λ .

(2) Let the input pattern be white noise, so that

$$\phi_{LL}(\omega) = N$$

or

$$\psi_{LL}(t) = 2\pi N \mu_0(t)$$

Substitution into Eq. (3) gives

$$R(\Delta t) = 2\pi N \left[\int_{-\infty}^{\infty} \mathbb{H}_{DF}(\eta) \mathbb{H}_{DF}(\eta - \Delta t) d\eta - \int_{-\infty}^{\infty} \mathbb{H}_{DH}(\eta) \mathbb{H}_{DF}(\eta - \Delta t) d\eta \right]$$

$$R(\Delta t) = 2\pi N [\psi_{FH}(\Delta t) - \psi_{HF}(\Delta t)]$$

where ψ_{FH} is the crosscorrelation function of $\mathbb{H}_{DF}(t)$ and $\mathbb{H}_{DH}(t)$ and ψ_{HF} is the crosscorrelation function between $\mathbb{H}_{DH}(t)$ and $\mathbb{H}_{DF}(t)$.

(3) Let the input pattern be sinusoidal and the D , F , and H filters have transfer functions of the form proposed by Reichardt. Then from Eqs. (5) and (8)

$$R(\Delta t) = \frac{b^2 b_{DF} b_{DH} \left(\frac{2\pi v}{\lambda}\right)^2 (a_H - a_F)}{\left[\left(\frac{2\pi v}{\lambda}\right)^2 + a_H^2\right] \left[\left(\frac{2\pi v}{\lambda}\right)^2 + a_F^2\right]} \sin \frac{2\pi \Delta s}{\lambda} \quad (9)$$

This expression suggests a set of experiments to estimate Δs , a_H , and a_F . If the reaction to sinusoidal patterns of various wavelengths is measured for various pattern velocities then each reaction curve should be "bell-shaped" as a function of velocity. The width of the "bell" is determined by a_H and a_F . Whether the "bell" is positive, negative, or zero is determined by the factor $\sin 2\pi \Delta s / \lambda$.

- (4) Finally, let the input pattern be a square wave and the D , F , and H filters have transfer functions of the form proposed by Reichardt. Then the input pattern can be represented by a Fourier cosine series as follows:

$$L(t) = \sum_{k=1,3,5,\dots}^{\infty} \frac{4b}{\pi k} (-1)^{\frac{k-1}{2}} \cos \frac{2\pi k}{\lambda} t.$$

Using Eq. (9)

$$R(\Delta t) = \sum_{k=1,3,5,\dots}^{\infty} \frac{\left(\frac{4b}{\pi k}\right)^2 b_{DF} b_{DH} \left(\frac{2\pi k v}{\lambda}\right)^2 (a_H - a_F)}{\left[\left(\frac{2\pi k v}{\lambda}\right)^2 + a_H^2\right] \left[\left(\frac{2\pi k v}{\lambda}\right)^2 + a_F^2\right]} \sin \frac{2\pi k \Delta s}{\lambda} \quad (10)$$

Since square wave patterns are easier to make than sinusoidal patterns, Eq. (10) is useful in predicting the output in a common experimental situation. Note that the maximum amplitude of the third harmonic component is only $1/9$ the maximum amplitude of the fundamental.

C. RUNNING AUTOCORRELATION

Up to now we have considered S filters in the two-ommatidia model to be perfect averagers. However, this is an approximation that can only apply to the steady state since, in general, the future as well as the past must be known to determine the average. A more accurate description of the S -filters, especially for the dynamic case, can be

made in terms of the running correlation function proposed by Licklider:⁹

$$\gamma_{12}(t, \tau) = \int_0^{\infty} f_1(t - T) f_2(t - T - \tau) W(T) dT$$

where $W(T)$ is a weighting or memory function.

Sayers and Cherry¹⁰ have used this function in modeling binaural fusion and have proposed a model for binaural fusion remarkably similar to Reichardt's two-ommatidia model.

Using the running correlation function, the weighting function of the S-filters in Fig. 7 becomes $W_S(t)$. Then Eq. (3) becomes

$$\begin{aligned} R(\Delta t, t) &= \int_0^{\infty} W_{DF}(\eta) \int_0^{\infty} W_{DH}(\zeta) \gamma_{LL}(t, \zeta + \Delta t - \eta) d\zeta d\eta \\ &\quad - \int_0^{\infty} W_{DH}(\eta) \int_0^{\infty} W_{DF}(\zeta) \gamma_{LL}(t, \zeta + \Delta t - \eta) d\zeta d\eta \end{aligned}$$

where

$$\gamma_{LL}(t, \zeta + \Delta t - \eta) = \int_0^{\infty} L(t - T - \eta) L(t - T - \Delta t - \zeta) W_S(T) dT \quad .$$

IV BEHAVIORAL EXPERIMENTS

A. TECHNIQUES AND EQUIPMENT

The beetles were mounted in position by gluing a piece of paper to pronotum and elytra as shown in Fig. 8. This paper was then fixed to a stand. The beetle *Lixus* has the characteristic that he will attempt to grasp any object with his legs if he is not flying or his legs are not touching the ground. Thus, the beetle will involuntarily hold the Y-maze globe, making it possible to measure the optomotor reaction to various visual patterns. The beetles were mounted so that they could not move the pronotum or elytra. However, the head was free to move.



FIG. 8 BEETLE AND Y-MAZE GLOBE AT THE CENTER OF A STRIPED CYLINDER

The Y-maze globe used in the experiments was made by cutting four equilateral, spherical triangles out of a ping-pong ball, leaving the edges of a spherical tetrahedron with smooth intersections. The patterns for the cylindrical drums were black and white strips printed on photographic paper. All of the patterns were made by carefully putting black electrical tape on a white board so that the width of a black stripe was equal to the width of a white stripe. Then a photograph was taken of the board. Black and white patterns of different wavelengths were obtained by varying the size of the enlargement that was printed on 18" by 20" photographic paper.

The cylindrical drums used to mount the striped patterns were made from transparent 6-inch OD lucite tubing. The pattern was mounted on the outside of the tubing.

The drums were rotated by a Bodine NSH-12 motor with SH-12 speed control. The speed of rotation was measured with a hand-held tachometer.

In the early experiments the responses were recorded by watching the beetle and marking the right and left turns on a data sheet. This proved to be unsatisfactory because of the close attention required and the rapid rate at which decisions were made.

An automatic counter for keeping track of the accumulated totals of right turns, left turns, right turns followed by right turns, right turns followed by left turns, left turns followed by left turns, and left turns followed by right turns was designed and built. In this device two light beams were positioned vertically behind the beetle so that one beam would be intersected by the Y-maze globe when a decision was made. The reflected light from the Y-maze globe was detected by two corresponding phototransistors, and this signal in turn activated relays that performed the necessary logic and energized the appropriate counters. A time delay circuit was employed so that decisions could not be made at shorter intervals than the time it took the beetle to walk from one intersection to the next. This circuit eliminated most of the extraneous signals from unwanted movements of the beetle between intersections.

B. SINGLE-CYLINDER EXPERIMENT

In one set of experiments the beetle was placed in the center of a striped cylinder. The direction of rotation, speed of rotation,

and stripe spacing were varied. There were at least 100 decisions at each speed with each stripe spacing. Figure 9 shows the results. Note that the 4° wavelength always gave a positive reaction, the 6° wavelength always gave a negative reaction, the 8° and 12° wavelengths gave reactions close to zero, and the 18° wavelength always gave a positive reaction.

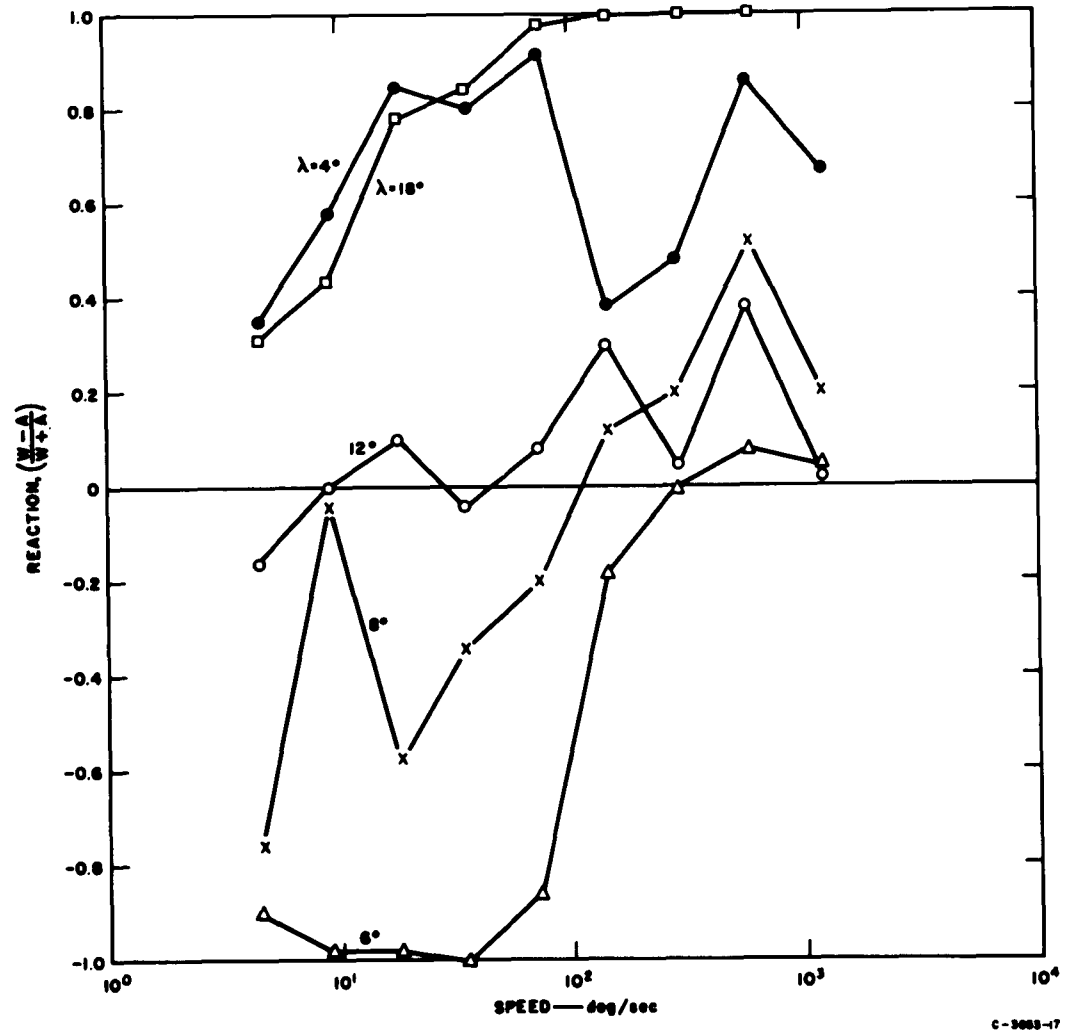


FIG. 9 REACTION VERSUS CYLINDER SPEED FOR VARIOUS BLACK AND WHITE STRIPE WAVELENGTHS

In another set of experiments a grating or mask was placed between the beetle and the cylinder. These results qualitatively agree with those above and will be reported in a later technical note.

C. DOUBLE-CYLINDER EXPERIMENT

Reichardt's double-ommatidia model predicts a zero reaction if both ommatidia receive the same signal as a function of time. This condition can be created experimentally with the apparatus shown in Fig. 10. In this situation, only one eye of the beetle is stimulated and each half of this eye is exposed to motion in an opposite direction. According to the model, the partial reactions of each half of the eye should cancel each other, resulting in zero reaction.

However, since two stripes moving away from each other create a similar two-dimensional projection similar to that of two stripes with a fixed separation moving toward the plane of projection, one might expect a turning response to this visual field. Thus, the double-cylinder experiment was aimed at determining if such a response existed.

Table I summarizes the results. While a slight but statistically significant reaction was obtained, this result can probably be attributed to a small misalignment in the apparatus. However, the results illustrate that each decision is not statistically independent of the previous decisions.

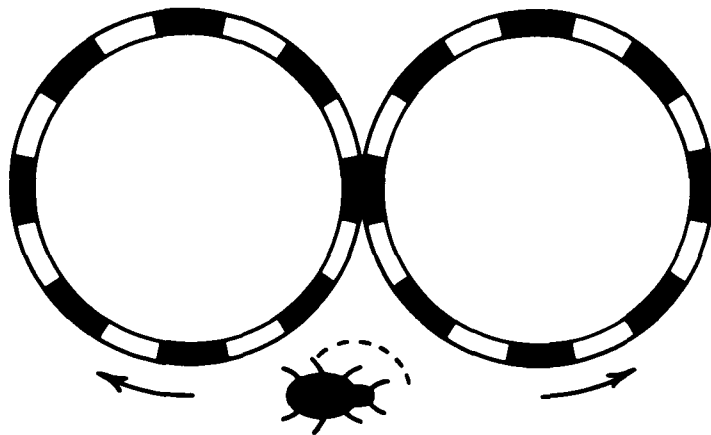


FIG. 10 EXPERIMENTAL SETUP FOR THE DOUBLE-CYLINDER EXPERIMENT

Table I
RESULTS OF THE DOUBLE-CYLINDER EXPERIMENT

DIRECTION OF CYLINDER ROTATION	ORIENTATION OF THE BEETLE	NUMBER OF DECISIONS IN EACH DIRECTION						PROBABILITIES					
		Left	Right	Left Followed by Left	Right Followed by Right	Left Followed by Right	Right Followed by Left	P(L)	P(R)	P(L/L)	P(R/R)	P(L/R)	P(R/L)
		327	451	189	329	128	124	0.42	0.58	0.58	0.73	0.28	0.38
		669	660	386	379	290	284	0.50	0.50	0.58	0.58	0.44	0.42
Totals		996	1111	575	708	418	408	0.46	0.54	0.58	0.64	0.38	0.41

D. DISCUSSION

The results of the single-cylinder experiment vary with changes in wavelength in accordance with Reichardt's model if an ommatidial angle of about 4° is assumed. This agrees well with the ommatidial angle found anatomically.

However, the relation between optomotor reaction and cylinder speed did not show the predicted behavior. A model that promises to take care of this difficulty is discussed in Sec. VI.

The double-drum experiment substantiated the assumption that the output of various parts of the eye is algebraically summed. It also showed that the sequential decisions are not statistically independent.

V ELECTRICAL RECORDINGS FROM THE BEETLE *LIXUS*

A. METHODS

The snout beetles *Lixus blakeae* Chittendan were used exclusively in the experiments. Prior to many of the experiments, the animals were anesthetized with carbon dioxide and immediately fixed to a preparation holder by means of Cenco "Tackiwax." No differences were noted between the responses of animals that received carbon dioxide and those that did not.

The microelectrode was placed in position with a Pfeiffer micro-manipulator while being viewed with a stereoscopic microscope. Either epoxy-coated, etched tungsten electrodes¹¹ or KCl-filled glass micropipettes¹² were used. The indifferent electrode was either a platinum or chlorinated silver wire.

A Bioelectronics Instruments DS2C amplifier and a Tektronix 502 oscilloscope were used to amplify and view the responses. The responses were recorded either by photographing the oscilloscope screen or with a Brush recorder.

B. THE ELECTRORETINOGRAM (ERG)

Vowles¹³ gives a review of the many studies on insect ERG. Perhaps the ERG study most closely related to the work described here is that of Kirschfeld.¹⁴

Several experiments were performed to establish the characteristics of the ERG in the beetle *Lixus*. In one set of these experiments a GR Strobotac light type 1531-A was used as the visual stimulus. This light source was placed two feet from the beetle in a dark room and produced the pulse shown in Fig. 11 in a 2N469A phototransistor circuit near the animal.

The electrical responses from the beetle were recorded from a glass micropipette filled with 3M KCl and having a resistance of about 15 megohms. This micropipette was placed in a small opening made on the dorsal margin of the eye with a sharp needle. The indifferent electrode was a chlorinated silver wire which was placed in an opening in the head-thoracic margin.

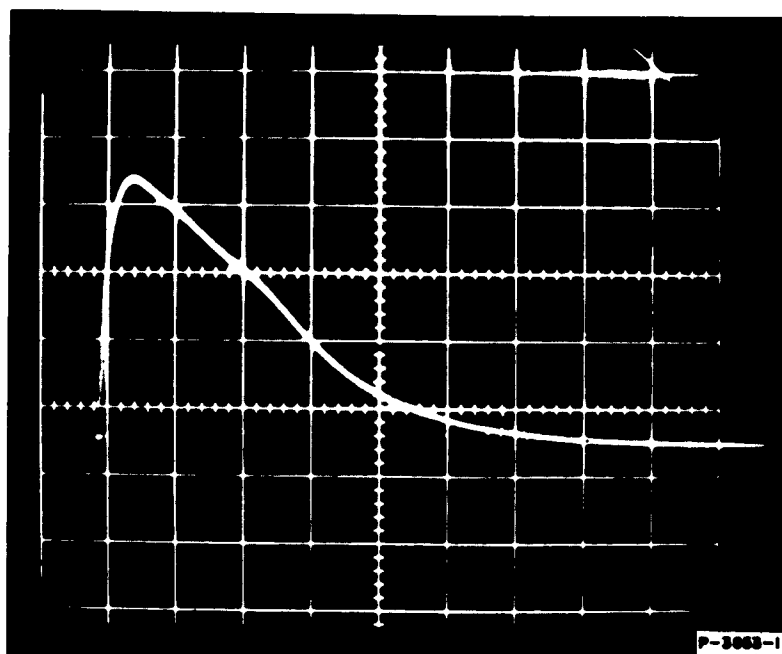
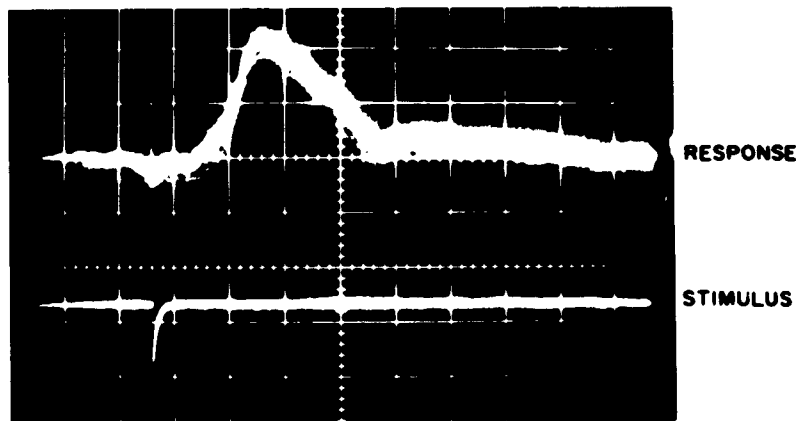
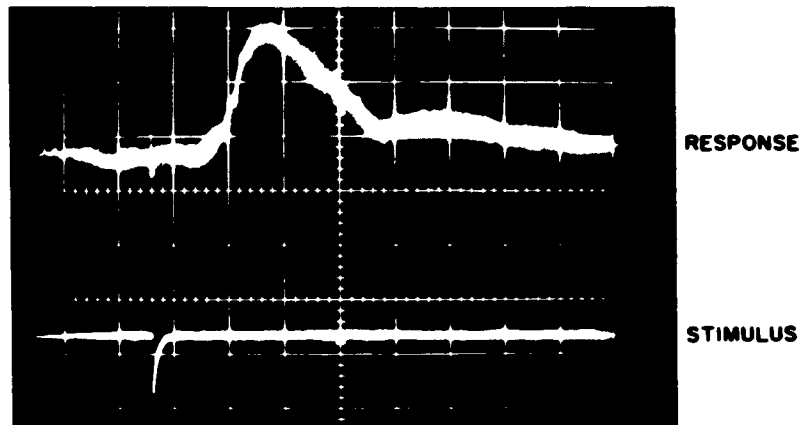


FIG. 11 STIMULUS LIGHT PULSE PRODUCED BY STROBOTAC.
HORIZONTAL SCALE: 20 μ sec/cm

Examples of the results are shown in Fig. 12 and 13 for two different pulse repetition frequencies. Note that there is a delay of approximately 16 msec followed by a positive potential with respect to the body. This latent period of approximately 16 msec is similar to that previously found by other investigators¹⁴ in arthropods. The time duration of this response is approximately 60 msec, and the rise time is much more rapid than the fall.

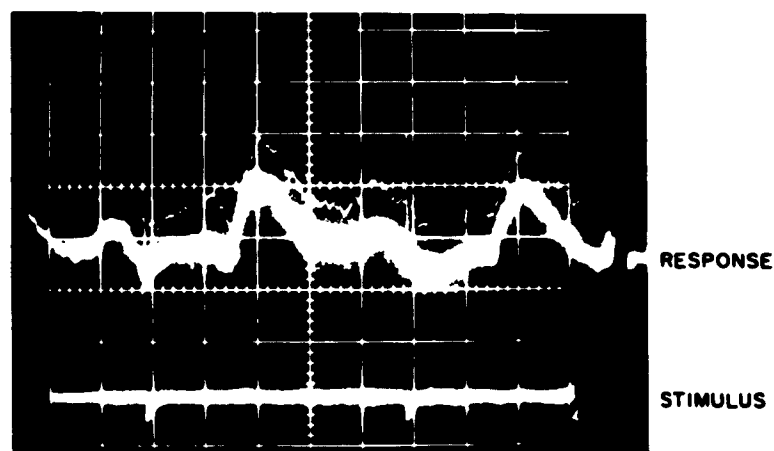
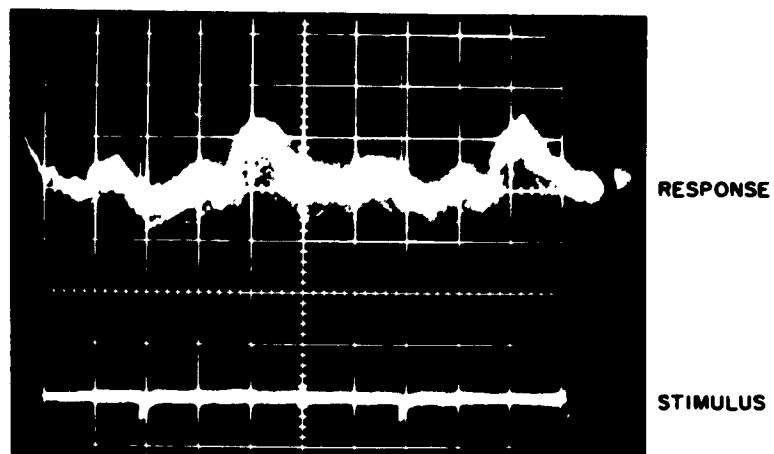
Responses to step changes in light intensity from a GE 1493 lamp were also noted in the same preparation. Figure 14 gives an example of the results. The response potential was positive going with respect to the body and appeared to differentiate the light stimulus.

In a second set of experiments, ERG responses to step changes in light intensity and triangular waves of light intensity were determined. In these experiments the tungsten microelectrodes were used with a platinum-indifferent electrode. A small hole (equal to several ommatidia in area) was made in the cornea with a sharp needle. The microelectrode was placed in this hole. The indifferent electrode was placed in the scutellum.



P-2003-2

FIG. 12 ERG RESPONSE TO STROBOTAC LIGHT PULSE FOR REPETITION FREQUENCY OF 100 PULSES PER MINUTE. HORIZONTAL SCALE: 20 msec/cm



P-3053-3

FIG. 13 ERG RESPONSE TO STROBOTAC LIGHT PULSE FOR PULSE REPETITION FREQUENCY OF 600 PULSES PER MINUTE. HORIZONTAL SCALE: 20 msec/cm

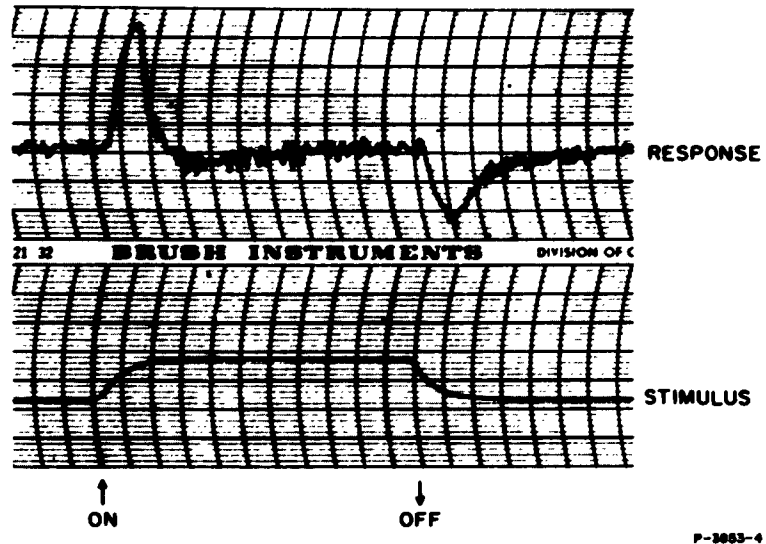


FIG. 14 ERG RESPONSE TO STEP CHANGE IN LIGHT INTENSITY. HORIZONTAL SCALE: 25 mm/sec (Glass micropipette in the dorsal margin of the eye)

Figure 15 shows an example of the response to a step change in light intensity. Note that in this case, unlike the case in which the electrode was in the dorsal margin of the eye, the corneal potential went negative with respect to the body when the light intensity was increased. The following parameters have been estimated from the results:

- | | |
|--|------------|
| (1) Time to reach 50 percent of the total potential change when the light is increased | = 50 msec |
| (2) Time to reach 50 percent of the total potential change when the light is decreased | = 150 msec |
| (3) Delay time for a response after an increase in light intensity | = 16 msec |
| (4) Delay time for a response after a decrease in light intensity | = 16 msec |

A triangular wave of light intensity was generated by transmitting light through a cylindrical sector of a rotating striped drum which encircled the preparation. The sector illuminated was equal in width to one stripe on the drum. Figures 16 and 17 show examples of the responses to this visual stimulus for different triangular wave frequencies.

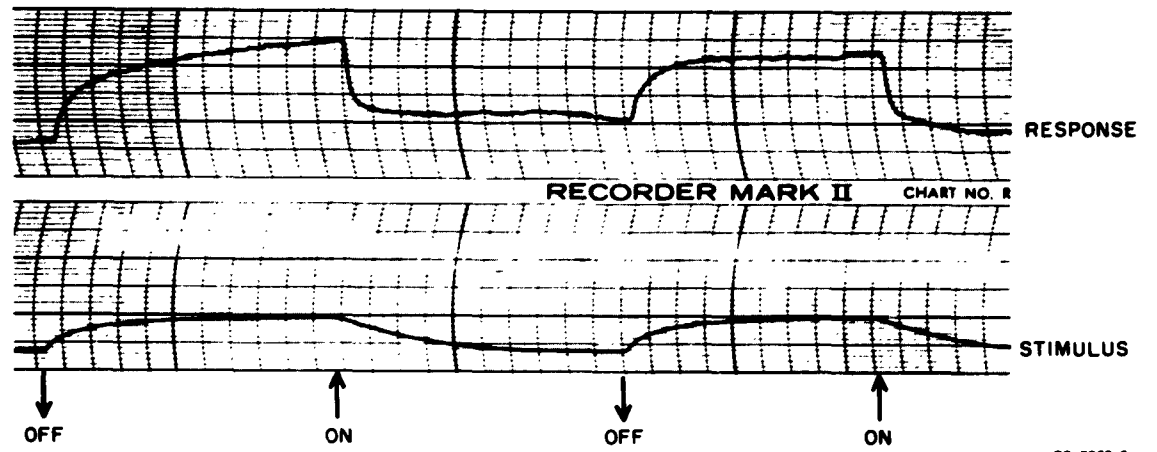


FIG. 15 ERG RESPONSE TO STEP CHANGE IN LIGHT INTENSITY. HORIZONTAL SCALE: 25 mm/sec (Tungsten microelectrode in the center of the eye)

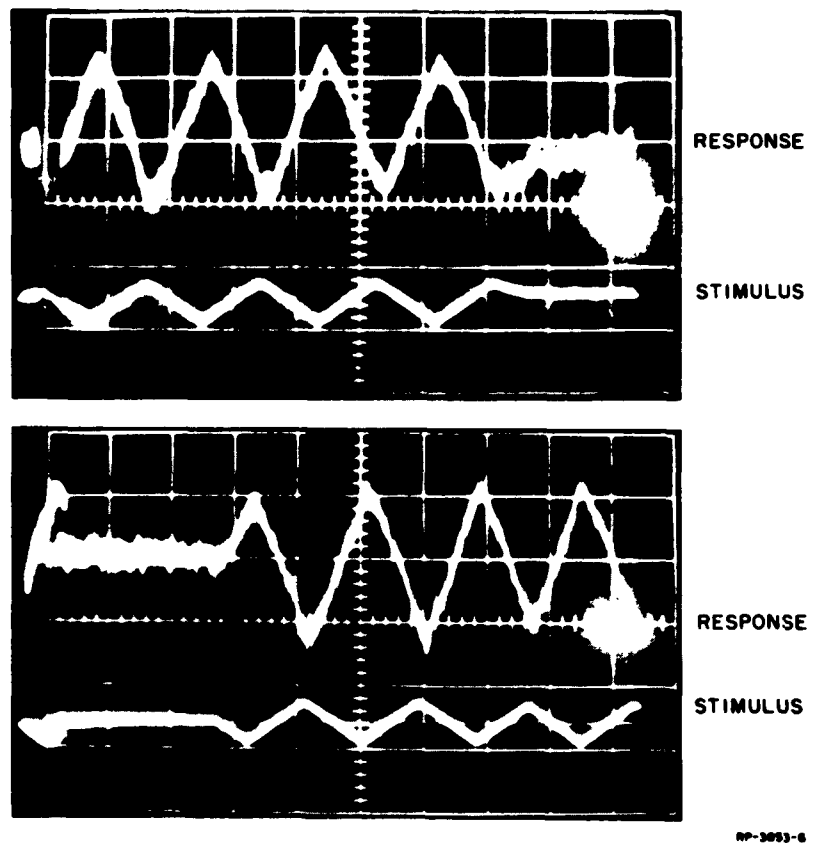


FIG. 16 ERG RESPONSE TO A TRIANGULAR WAVE OF LIGHT INTENSITY. HORIZONTAL SCALE: 500 msec/cm

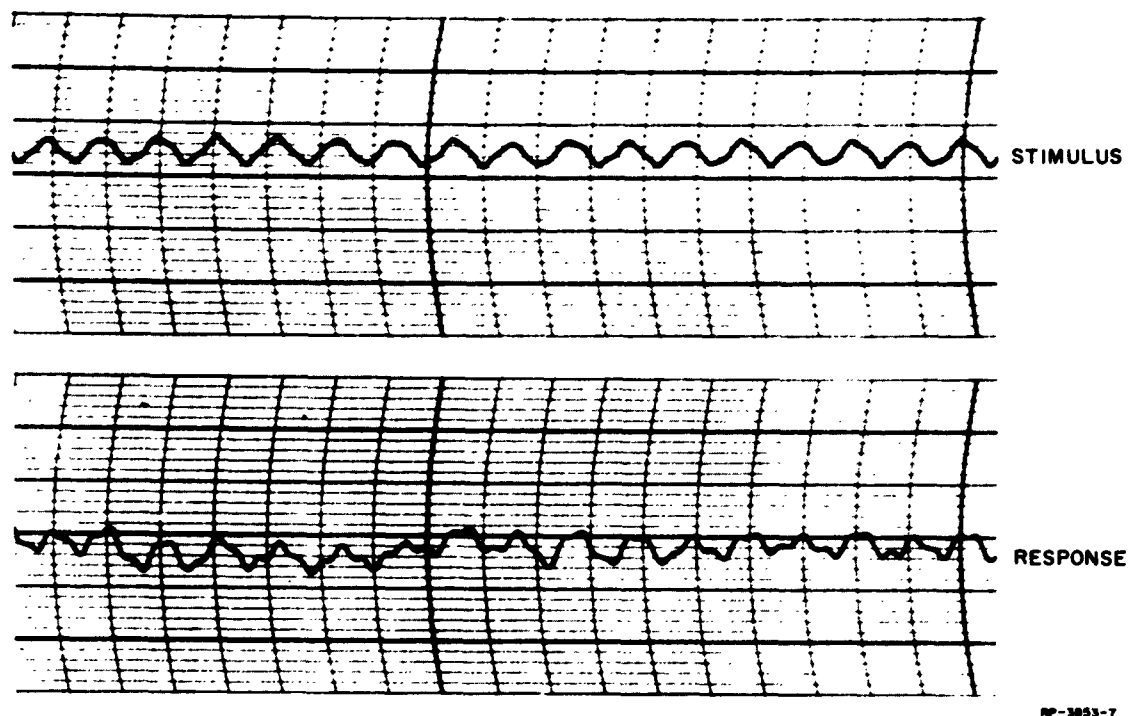


FIG. 17 ERG RESPONSE TO A TRIANGULAR WAVE OF LIGHT INTENSITY.
HORIZONTAL SCALE: 125 mm/sec

Figure 18 shows a plot of the amplitude of the triangular wave responses versus frequency for two experimental runs. Also plotted on the same graph are the results reported by Kirschfeld for *Hylobius*.

It can be seen from these curves that the amplitude versus frequency response approximates a single lag of 6 db/octave with a corner frequency at approximately 4 cps.

Figure 19 gives the phase of the response with respect to the triangular wave light stimulus as a function at frequency. Note that if a 13 msec pure delay is subtracted from this phase characteristic, the pulse never exceeds 90 degrees, the minimum phase shift producible by a single lag network. Figure 20 gives an electrical network that approximates this ERG data for *Lixus*.

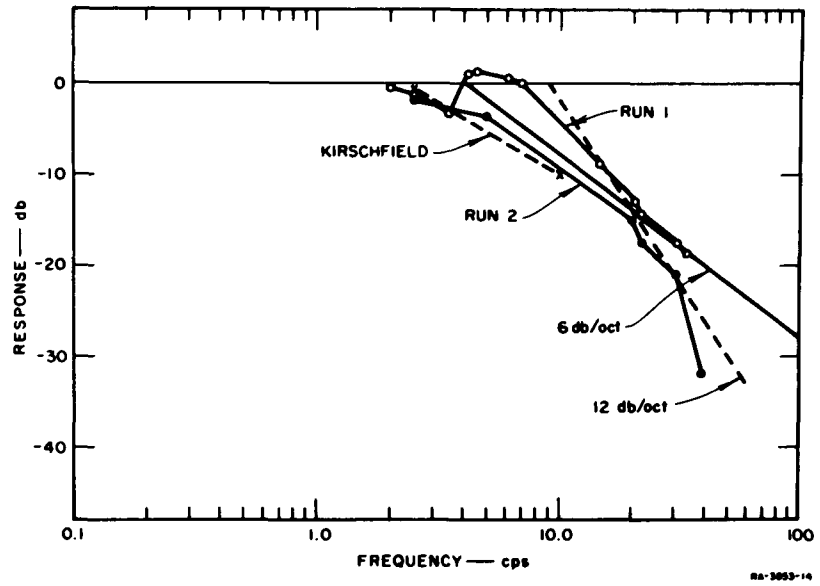


FIG. 18 AMPLITUDE OF THE TRIANGULAR WAVE ERG RESPONSE VERSUS FREQUENCY FOR TWO EXPERIMENTAL RUNS

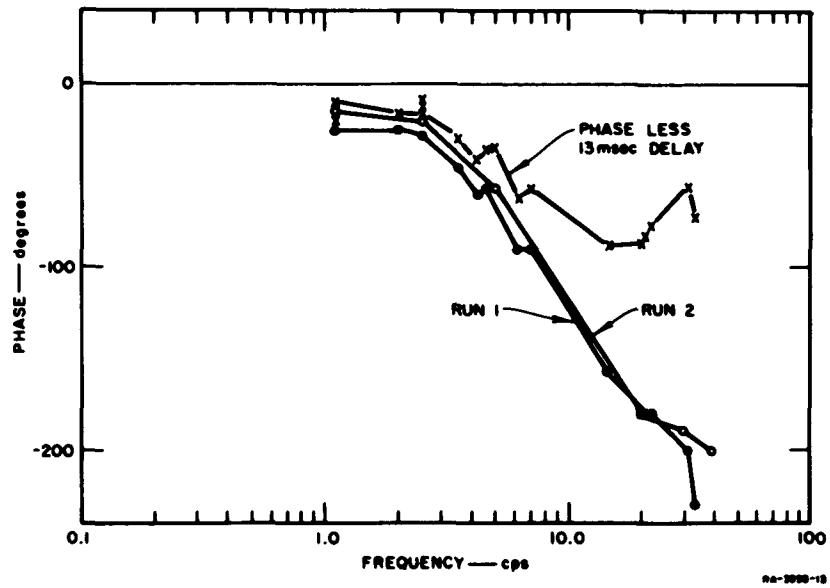
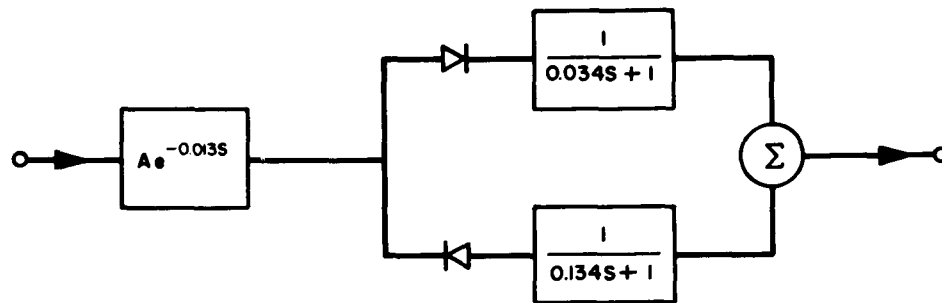


FIG. 19 PHASE OF THE TRIANGULAR WAVE ERG RESPONSE VERSUS FREQUENCY FOR TWO EXPERIMENTAL RUNS

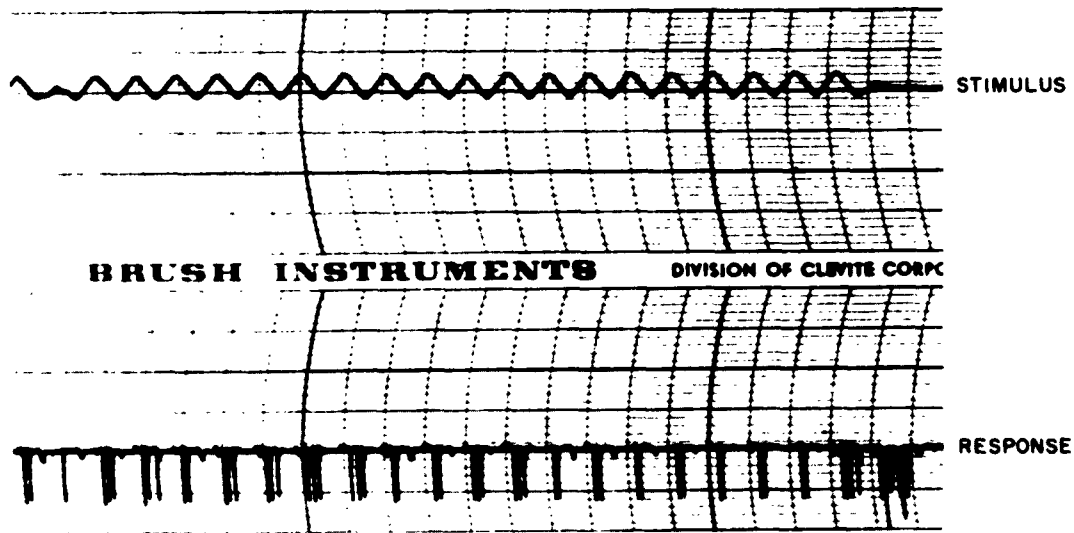


A-3055-II

FIG. 20 ELECTRICAL NETWORK THAT APPROXIMATES THE ERG RESPONSE

C. SPIKE POTENTIALS

Several methods for obtaining spike potentials in the beetle *Lixus* have been found. In one experiment a tungsten electrode was placed in a small hole in the cornea. Figure 21 shows the spike response, apparently from a single cell, to a triangular-wave light stimulus. Note that the bursts of two or three spikes occur in synchronism with the increases in light intensity, each burst starting approximately



RP-3053-12

FIG. 21 SPIKE RESPONSE TO A TRIANGULAR WAVE OF LIGHT STIMULUS.
HORIZONTAL SCALE: 5 mm/sec

100 milliseecs after the peak of the triangular wave. It was also noted that if the intensity of the light increases were decreased, the number of spikes on each burst decreased. Other experiments indicated that the cell seemed to respond only to an increase in light intensity. The amount of increase was coded into number of spikes in a burst and the rate of change was coded into the time duration between spikes.

Figure 22 shows a plot of the rate of increase of the stimulus light intensity versus the reciprocal of the time between pulses.

Spike potentials have also been obtained with the glass micro-pipettes in the ventral nerve cord, anterior thoracic region, and motor nerve stump of the first joint of the right front leg. In most of these records no apparent correlation to simple light stimuli was noted. However, they indicate the possibility of obtaining motor nerve responses that could correlate with turning tendency in the behavioral experiment.

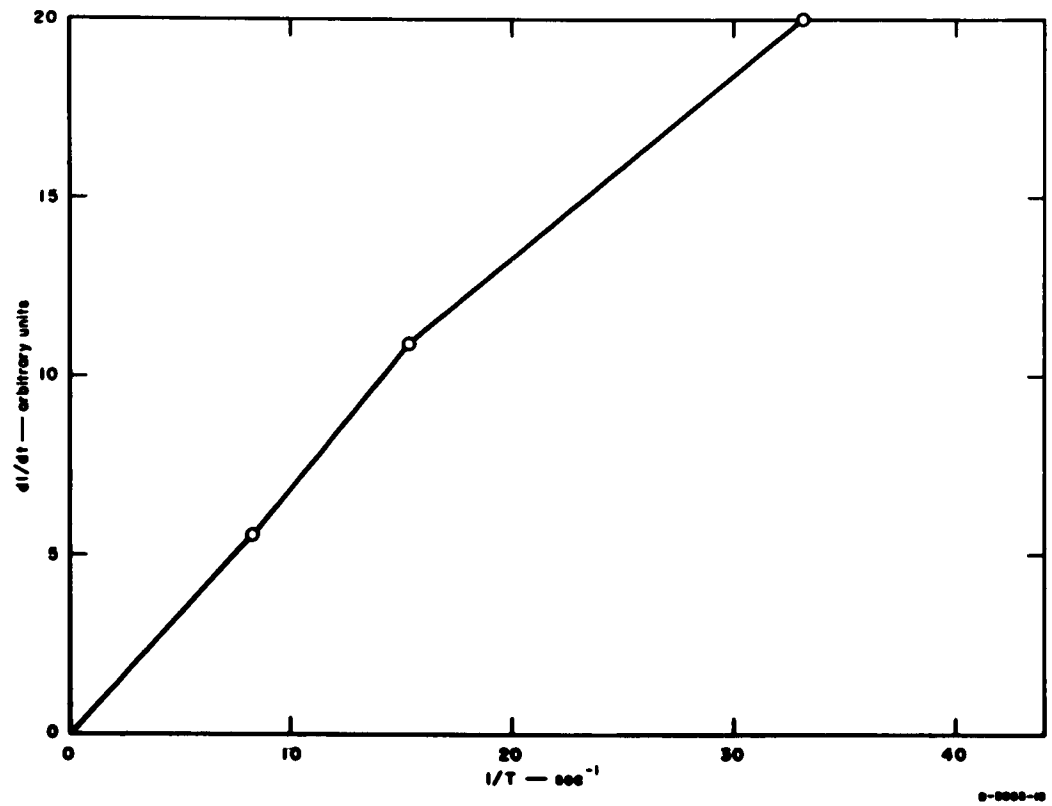


FIG. 22 RATE OF INCREASE OF THE STIMULUS LIGHT INTENSITY
VERSUS THE RECIPROCAL OF THE TIME BETWEEN PULSES

VI CONCLUSIONS

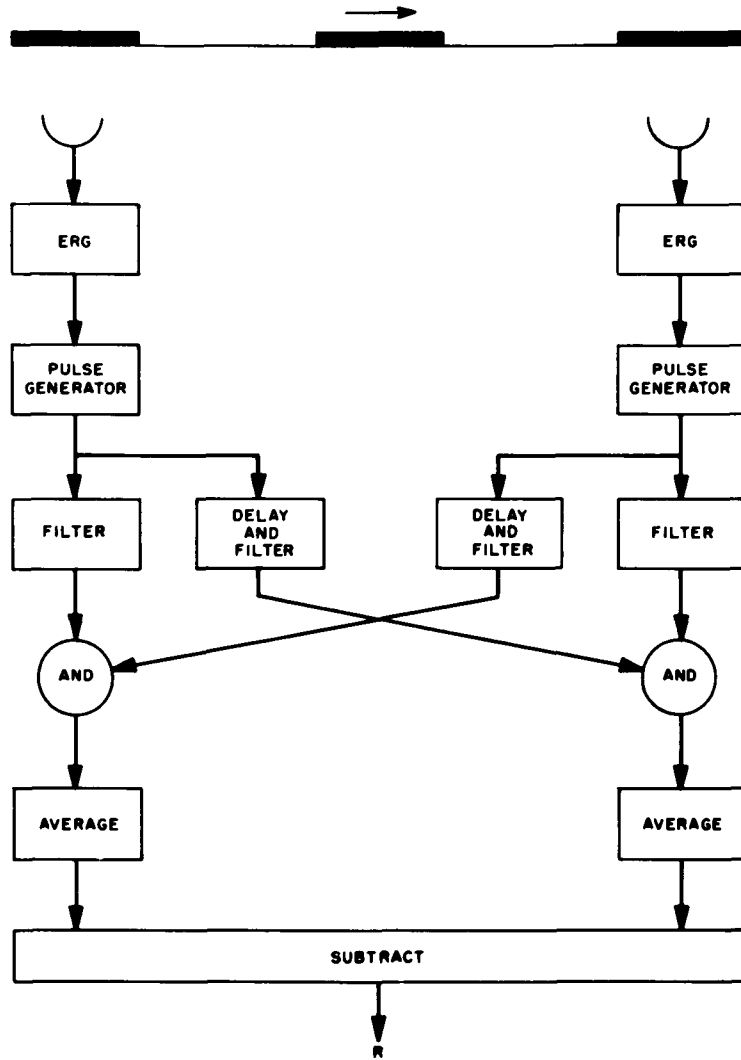
The major results obtained were:

- (1) Anatomically, the angle between center-lines of adjacent ommatidia was determined to be about 4° .
- (2) Reichardt's model of a horizontal section of the eye of the beetle *Chlorophanus* resembles an autocorrelation computer in which the output is the sum of the autocorrelation coefficient with no shift and the autocorrelation coefficient with a shift of one ommatidial angle.
- (3) A Fourier Spectral Density Computer can be used to calculate the same output as Reichardt's model of a horizontal section without the use of multipliers.
- (4) It is shown that Reichardt's two-ommatidial model computes a function of the autocorrelation function of the input pattern, and a synthesis procedure is given that determines filter functions for a particular function of the autocorrelation function.
- (5) A modification of Reichardt's two-ommatidial model is suggested to take account of dynamic phenomena. A running autocorrelation is suggested instead of a perfect averager.
- (6) Equipment was developed that automatically accumulates the results of behavioral experiments that use a Y-maze globe.
- (7) The results of the single-cylinder experiment vary with changes in wavelength in accordance with Reichardt's two-ommatidial model if an ommatidial angle of about 4° is assumed.
- (8) The "bell-shaped" reaction as a function of pattern speed predicted by Reichardt's model was not obtained.
- (9) The results of a double-cylinder experiment were in agreement with the assumption that the partial reactions of ommatidial pairs are summed.
- (10) The results of the Y-maze globe experiments showed that sequential decisions were not statistically independent.
- (11) An ERG study demonstrated the nonlinearity of this response and suggested a 13 msec pure delay and a simple lag network with corner frequency at 4 cps as an approximation for the response to small changes in light intensity.

- (12) Spike potentials were obtained from a single cell that fired with an increase in light intensity.
- (13) Spike potentials were obtained from the ventral nerve cord, anterior thoracic region, and motor nerve stump of the first joint of the right front leg.

Results 8 and 12 above suggest that a model such as the one shown in Fig. 23 might better describe both the typographical and typological aspects of the two-ommatidial system. In this model it is first postulated that the input light pattern (the average light intensity over the ommatidial angle) is functionally filtered according to the dynamics of the ERG response. This response in turn drives a pulse generator which produces spikes in accordance with result 12. After filtering and delay, an output of an ommatidial channel together with an output of an adjacent channel is required to produce a signal which is averaged. Adjacent averages are subtracted producing the final reaction *R*.

This model suggests that for different levels of illumination the output should have a different character as a function of pattern speed. If the illumination is low, so that with each stripe only one pulse is generated, then a simple "bell-shaped" reaction as a function of pattern speed is obtained. However, if the illumination is high, so that several pulses are generated with each stripe, then a more complicated reaction with several maxima and minima is obtained. While this model has the correct qualitative behavior to explain our behavioral results, additional experimentation is necessary to establish its validity.



98-3093-10

FIG. 23 MODEL OF THE TWO-OMMATIDIA SYSTEM

REFERENCES

1. Roeder, K. D., "A Physiological Approach to the Relation Between Prey and Predator," *Smithsonian Miscellaneous Collections*, 137, pp. 287-311, 1959.
2. Vowles, D. M., "Neural Mechanisms in Insect Behavior," W. H. Thorpe and O. L. Zangwill, Eds., of *Some Problems in Animal Behavior*, pp. 5-29 (Cambridge University Press, 1961).
3. Hassenstein, B., "Optokinetische Wirksamkeit bewegter periodischer Muster," (Nachmessungen am Russelkäfer *Chlorophanus viridis*), *Z. Naturforschung*, 14b, pp. 659-674 (1959).
4. Reichardt, W., "Autocorrelation, a Principle for the Evaluation of Sensory Information by the Central Nervous System," in *Sensory Communication*, edited by W. A. Rosenblith, MIT Press and John Wiley & Sons, Inc. (1961) pp. 303-318.
5. Reichardt, W., "Nervous Integration in the Facet Eye," *Biophysical Journal*, 2, No. 2, Part 2, suppl. pp. 121-143, 1962.
6. Varju, D., "Optomotorische Reaktionen auf die Bewegung periodischer Helligkeitsmuster," *Z. Naturforsch.*, 14b, pp. 725-734, 1959.
7. Miller, Raymond J., "Air and Space Navigation System Using Cross-Correlated Detection Techniques," *Electronics* 34, No. 50, pp. 55-59 (5 December 1961).
8. Mason, S. J. and H. J. Zimmerman, *Electronic Circuits, Signals, and Systems*, (John Wiley & Sons, Inc., New York, 1960) pp. 350-354.
9. Licklider, J. C. R., "A Duplex Theory of Pitch Perception," *Experiments*, 7, pp. 128-131 (1951).
10. Sayers, B., and C. Cherry, "Mechanism of Binaural Fusion and the Hearing of Speech," *JASA*, 29 Sept. 1957, pp. 975-987.
11. Hubel, D. H., "Tungsten Microelectrode for Recording from Single Units," *Science*, 125, pp. 549-550, March 22, 1957.
12. Donaldson, P. E. K., *Electronic Apparatus for Biological Research*, (Butterworths Scientific Publications, London, 1958) pp. 534-567.
13. Vowles, D. M., "The Physiology of the Insect Nervous System," pp. 349-373 in *International Review of Neurobiology*, 3, Academic Press, New York (1961).
14. Kirschfeld, K., "Quantitative Beziehungen Zwischen Lichtreiz und Monophasischem Elektretinogramm Bei Russelkäfern," *Z. Vergleichende Physiologie*, 44, pp. 371-413, 1961.

ACKNOWLEDGMENT

The author wishes to acknowledge Dr. Glen Haydon and Miss Carol Foster of the Life Sciences Division of Stanford Research Institute for their preparation of the section of the beetle head, Mr. Alan Adolph of the Rockefeller Institute for his advice and help on the microelectrode recordings, Prof. Ray F. Smith of the University of California for identifying the beetles, Mr. Thomas Kittredge for his help with the experiments and the care of the beetles, and Messrs. Brian King and James Willis for the development of the automatic equipment for the behavioral experiments.

PROJECT STAFF ACTIVITIES

Meeting Papers Presented

James C. Bliss, "Visual Information Processing in the Beetle *Lixus*," presented at the Symposium on Optical Processing of Information, October 23, 24, 1962, Washington, D. C.

James C. Bliss, "Tactual-Kinesthetic Perception of Information," presented at the International Congress on Technology and Blindness, June 18-22, 1962, New York, New York.

Papers Published

James C. Bliss, "Kinesthetic-Tactile Communications," *IRE Trans., IT-8*, No. 2, pp. 92-98 (February 1962).

James C. Bliss and William B. Macurdy, "Linear Models for Contrast Phenomena," *J. Optical Soc. Am.*, Vol. 51, No. 12, pp. 1373-1379, (December 1961).

Papers Accepted for Publication

James C. Bliss, "Information Presentation to the Tactile and Kinesthetic Senses," Chapter 24 of *Human Factors in Electronics*, McGraw-Hill, 1962.

Lectures

James C. Bliss, "Biocommunications," Graduate Electrical Engineering Course taught at Stanford University, 1962.

James C. Bliss, "Visual Information Processing," Seminar given at the California Institute of Technology, May 1962.

**STANFORD
RESEARCH
INSTITUTE**

**MENLO PARK
CALIFORNIA**

Regional Offices and Laboratories

Southern California Laboratories

820 Mission Street
South Pasadena, California

Washington Office

808 17th Street, N.W.
Washington 5, D.C.

New York Office

270 Park Avenue, Room 1770
New York 17, New York

Detroit Office

The Stevens Building
1025 East Maple Road
Birmingham, Michigan

European Office

Pelikanstrasse 37
Zurich 1, Switzerland

Japan Office

911 Iino Building
22, 2-chome, Uchisaiwai-cho, Chiyoda-ku
Tokyo, Japan

Representatives

Honolulu, Hawaii

Finance Factors Building
195 South King Street
Honolulu, Hawaii

London, England

19 Upper Brook Street
London, W. 1, England

Milan, Italy

Via Macedonio Melloni 40
Milano, Italy

London, Ontario, Canada

P.O. Box 782
London, Ontario, Canada